Collisionless Plasma Astrophysics Simulation Experiments using Lasers

N. C. Woolsey, A. D. Ash, C. Courtois*, R. O. Dendy[1], C. D. Gregory, I. M. Hall and J. Howe

Department of Physics, University of York, York, Y010 5DD, United Kingdom
[1] UKAEA Culham Division, Culham Science Centre, Abingdon, OX14 3DB, United Kingdom

Abstract. Laboratory experiment is an attractive method of exploring the plasma physics that may occur in solar and astrophysical shocks. An experiment enables repeated and detailed measurements of a plasma as the input conditions are adjusted. To form a scaled experiment of an astrophysical shock a plasma physics model of the shock is required, and the important dimensionless parameters identified and reproduced in the laboratory. A laboratory simulation of a young supernova remnant is described. The experiment uses the interaction of two millimetre-sized counter-streaming laser-produced plasmas placed in a strong transverse magnetic field to achieve this scaling. The collision-free dynamics of the two plasmas and their interaction are studied with and without the magnetic field through spatially and temporally resolved optical measurements. Laboratory astroplasma physics experiments using high-energy, high-power laser technology enables us to reproduce in the laboratory the conditions of temperature and pressure that are met in extreme stellar environments.

Keywords: Laser-produced-plasma; Shocks; Supernova remnants; Strong magnetic fields
PACS: 52.35.Tc, 52.38.-r , 52.25.Xz, 96.50.Fm, 98.58.Mj; 07.55.Db

INTRODUCTION

The use of large laser systems to model space and astrophysical plasma phenomena has been of interest since the mid-1960's [1], and since this time laser plasma experiments have provided fundamental information from spectroscopic data to equation of state measurements. With the development of facilities, target and diagnostic design, experiments have become more ambitious and have moved towards near complete experimental plasma simulations of astrophysical systems. The most advanced high-power laser-plasma simulations are associated with hydrodynamic processes [2, 3, 4] in supernovae and supernova remnants (SNRs) plasmas. These experiments require careful scaling to ensure that a number of dimensionless parameters [5] that describe the astrophysical object are reproduced in the laboratory. Through careful matching of these parameters it is possible to ensure that the laboratory experiment temporally evolves like the astrophysical object [6]. In addition, experiment can test or validate sophisticated multi-dimensional computer models [7]. These experimental simulations address complex phenomena that occur on the large scale where the hydrodynamic approximation holds, however they cannot address

CP827, *Superstrong Fields in Plasmas: Third International Conference on Superstrong Fields in Plasmas*, edited by D. Batani and M. Lontano

additional complex plasma physics processes such as wave-particle phenomena. Wave-particle interactions on the small scale influence large scale plasma dynamics, and are responsible for seeding and acceleration of cosmic rays; these subjects are of great interest to a broad section of the astrophysics community. The formation of collisionless plasmas and collisionless shocks similar to those typical of a SNR is the focus of this work [8,9,10,11]. Of particular interest is a young SNR of age 100 years, as these systems are believed to be particularly active sources of cosmic rays.

SNR ejecta is supersonic (and super-Alfvénic) and consists of relatively cold material with significant kinetic energy. On impacting the circumstellar and then interstellar material forward and reverse shocks form, separated by a contact interface. Both shocks are active regions of particle acceleration. An outstanding question associated with particle acceleration at these shocks includes identifying mechanisms for injection of background electrons and ions and acceleration to mildly relativistic levels. As the plasmas are collisionless, injection is likely to be collisionless.

General experiments [8,11,12,13] using collisionless plasmas have been proposed which may be able to address some of these complex collisionless plasma shock formation and wave-particle questions. In these experiments the relevant scale lengths must be the particle Larmor radii rather than a particle collisional mean-free-path, which constrains experimental design [14].

The absolute values of length, time, and density in SNRs greatly exceed those possible in an experiment; for a laboratory experiment to function as a simulation it must be correctly scaled. Scaling used here is based on ideal magnetohydrodynamics (MHD) and a polytropic equation of state [5,6]. Application of an ideal MHD model requires that plasma dissipation processes, as measured by the Reynolds Re and Péclet Pe numbers, be negligible. Large Re (10^{13}) and Pe (10^{11}) are found in SNRs [15] and imply negligible viscosity and thermal diffusivity respectively. Dissipative structures such as shocks are scaled in MHD, although the dissipative mechanisms within the shock are not.

Such ideal plasmas can be formed in laser-plasma experiments. The next step to a scaled experiment is to identify a set of fundamental dimensionless parameters that describe the SNR and ensure these are reproduced in the experiment. There are four essential dimensionless parameters. These are the plasma collisionality (ξ), the plasma-β ($= 2\mu_0 p/B^2$), the Euler number ($Eu = v(\rho/p)^{1/2}$), and the Mach numbers (M, and M_A). Where v is a characteristic velocity of the system, p is the plasma pressure, ρ is the mass density, μ_0 is permeability of free space, and B the amplitude of the magnetic field. The ξ is the ratio of the particle mean-free-path (MFP) to the scale length of interest, for example the shock thickness; in a SNR $\xi > 10^6$. The β and Eu parameters determine the MHD character of the system. Indicative values of β and Eu for a young SNR are 500 and 18 respectively [15]. A particular feature of a SNR is the large plasma-β [15]. A $\beta > 1$ indicates that the magnetic field does not directly affect the plasma dynamics, but in collisionless plasma reduces the length scales over which fluid behaviour occurs from the particle MFP's to the particle Larmor radii. Furthermore, for plasma to be considered an MHD fluid the Larmor radii need to be shorter than the scale of the features of interest, i.e. in this case the shock. This is believed the case in SNRs. A young SNR is characterized by strong shocks with hydrodynamic Mach and Alfvén Mach numbers of order 16 and 300 respectively.

COLLISIONLESS PLASMA EXPERIMENTS

The experimental designed is to converge on the physics relevant to a young SNR, rather follow the evolution. The account given here is a summary of material published elsewhere [8,9,10]. The SNR simulations are based on laser ablation of two low mass and low atomic number plastic (C_8H_8) foil targets. The ablation plasmas expand at high (supersonic) speed. A collision free interaction between the two plasmas is achieved by counter-propagating the two flows and carefully adjusting the initial separation between them. The 100 nm thick plastic foils are mounted face-parallel and typically separated by 1 mm as illustrated in Figure 1. The foil targets explode following uniform irradiation over a 1 mm diameter focal spot by a 1.053 μm wavelength laser with irradiance of 5×10^{13} W/cm^2 (± 10 %) in an 80 ps pulse. The laser intensity is sufficiently low to limit hot electron generation, yet significantly ionise the targets. The pulse duration is short to prevent self-generated magnetic fields at the time when the counter-flowing plasmas collide approximately 500 ps later. A focal spot diameter of twice the distance to the interaction point allows the plasma to be approximated as a 1-dimensional planar expansion with some confidence; this assumption simplifies the data analysis. The experiments are repeatable and the foil target thickness and separation may be varied to achieve the required scaling parameters. To achieve the required plasma-β it is necessary to apply an external field across the experiment, this is one of the more controversial and experimentally challenging aspects of the experiment. We have used a conventional pulsed Bitter electromagnet to generate a 7.5 T field for approximately 1 ms over a 10 mm region, and explored using laser-driven electromagnets which generates similar fields [9,16]. Both magnets were used in a Helmholtz coil configuration to ensure field uniformity across the experiment. A schematic of the experiment is shown in Fig. 1. The plasma flow is perpendicular to the magnetic field direction.

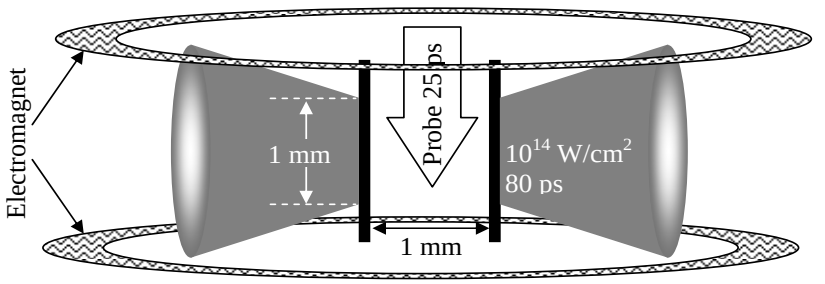

FIGURE 1. The typical foil target geometry, electromagnet setup and laser probe alignment. The probe is delayed relative to the peak of the drive lasers, by up to 1 ns.

The peak magnetic field is limited by the technology used; this restricts the plasma parameters experimentally accessible. The magnetic field should be sufficiently large to ensure that the electron and ion Larmor radii are the shortest length scales of physical relevance and are small compared to the spatial extent of the experiment, whilst the plasma-β exceeds unity. The later constraint ensures the plasma thermal energy dominates the magnetic energy.

Experiments are diagnosed with two-dimensional time-resolved optical probing, optical spectroscopy and ion time-of-flight measurements. A 25 ps duration, 0.53 μm wavelength optical probe was used for shadowgraph, schlieren and interferometric measurements. The probe was delayed from 0 – 1 ns after exploding the two foils so that the plasma density distribution and evolution can be inferred. Interferometry was sensitive to electron density minimum of 5×10^{17} cm^{-3} and maximum of 5×10^{19} cm^{-3} along an approximately 1-mm path through the plasma. The plasma temperature is inferred from the expansion speed, ion time-of-flight measurements and spatially resolved optical spectroscopy of Doppler broadened helium-like carbon (C^{4+}) transition lines $1s2s\ ^3S_1$ - $1s2p\ ^3P_{2,1,0}$ triplet transition centred at 227 nm.

These lines can also be used to measure the magnetic field in the plasma if the Zeeman splitting [17] exceeds the Doppler width. In addition, the magnetic field can be inferred from Faraday rotation of a polarised beam and from induction coil measurements. These methods were not sensitive enough to measure the magnetic field in the plasma in these experiments. The magnetic field was measured using 1 mm diameter, single turn induction coils connected to a 4 GHz analogue bandwidth oscilloscope. The induction coils were screened from energetic particles and placed approximately 10 cm from the target

Exploding plasma density non-uniformities resulting from structure imprinted by the laser beams, or from structure on the plastic foils may influence the interaction of the counter streaming plasmas, and impair the optical measurements. To limit beam imprint two or three beams were overlapped on each foil target, and random phase zone plates [18] were used to provide a super-Gaussian intensity profile across the 1 mm diameter laser focus. An additional set of experiments used a low energy spatially smoothed prepulse to preform a uniform plasma, this preformed plasma was then driven to expansion speeds using the high energy beams focussed with the phase zone plates [19].

Electron density profiles extracted from the interferometric data indicate that the plasma expansion speed at 500 ps after the peak of the 80 ps laser pulse (with 10% accuracy) is 1.1×10^8 cm/s. Measurement of single expanding plasmas in a 7.5 T magnetic field shows that the magnetic field does not affect the plasma expansion. This is illustrated by the electron density profiles in Fig. 2a; these results were inferred from interferometric measurements 750 ps into the experiment and confirm expectations as the plasma-β is large. Data analysis of interferometric results is discussed in detail in Ref. [20]. These results when combined with the low density and low atomic number ensure a collision-free interaction in a counter-streaming geometry. For fully ionised carbon (C^{6+}) the counter-flowing MFP, which scales as $1/Z^4$, exceeds 10 cm. The low plasma density is achieved by limiting the thickness of the foil targets to 100 nm, and in addition, can be adjusted by varying the foil target separation. An example of the type of data collected during the collision of two similar plasmas is shown in Fig. 2b. Lasers irradiate foil targets at -0.5 and 0.5 mm, and the interferometry image is recorded at 500 ps. The inferred n_e data suggests interpenetrating flow and has been compared to one-dimensional simulation. The simulation of two interpenetrating plasmas is derived by reflecting an experimental profile of a single exploding foil at 0.0 and adding the two results. The comparison

gives confidence that any interaction during the interpenetrating flow is small and can not be measured.

On applying a magnet field to a similar colliding plasma experiment the results are qualitatively different to those measured and simulated. This is illustrated by Fig. 2c. In this figure the n_e profile discussed above is compared to the n_e density profile with a 7.5 T magnetic field present. The shape of the n_e profile and not absolute n_e is of interest. Experiment illustrates that 10% variation in foil target thickness and laser intensity result in significant changes in the n_e at the collision point. We observe a steepened n_e profile close to the foil targets' initial positions separated by an approximately 300 μm wide low-gradient region centred on the collision point.

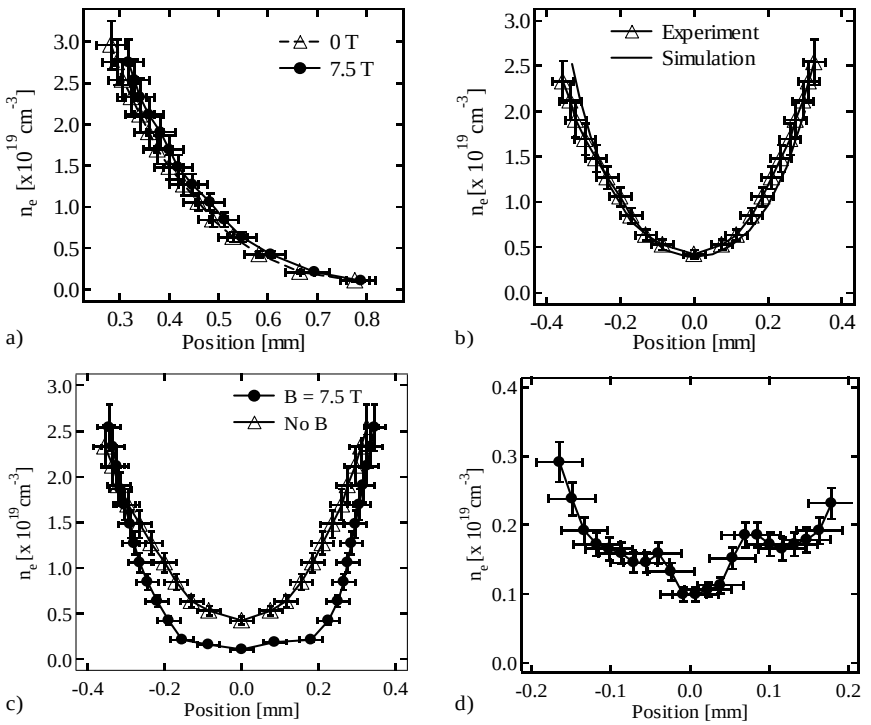

FIGURE 2. a) The inferred electron densities (n_e) taken from the central region of a single exploding 100 nm foil at 750 ps. The data indicates that a magnetic field does not affect the plasma expansion. b) The inferred n_e at 500 ps from two colliding plasmas, original target positions at -0.5 and +0.5 mm. Comparison with hydrodynamic simulation indicates the interaction is collision free. c) A comparison of inferred n_e at 500 ps for two similar experiments, with a 7.5 T field imposed on one experiment. The shape of the n_e profiles, not the absolute n_e are important. d) A more detailed examination of the n_e profile in a 7.5 T field close to the collision point.

We have sufficient data to exclude variation in experimental parameters (foil target thickness, separation, laser energy and balance) and must conclude this profile change results from an externally imposed magnetic field. Furthermore, similar data have been obtained using both the conventional and laser-driven electromagnets. We have

been unable observe these features evolve and it is noted that a shock has not been observed. Close inspection of the interferometry and n_e profiles, see Fig. 2d, suggest two additional density features are present in the low-density region centred on the collision point. These features have widths around 150 μm.

DISCUSSION

These experiments are a significant step towards the generation of a scaled and sustained collisionless shock. The potential for scaled simulation of a young SNR can be examined by comparing experimental values of the four scaling parameters that characterise the young SNR. Further applicability of the experiment is explored with numerical simulation. First, to apply MHD scaling it is essential that the plasma can be considered ideal and that a polytropic equation of state can be applied with some degree of confidence. Based on measurement we find that dissipation is negligible with high Reynolds ($R_e \sim 10^7$) and Péclet ($P_e \sim 10^{10}$) numbers. A fully ionised experimental plasmas, hence polytropic equation of state, is assumed given the laser irradiance (10^{14} W/cm^2) and the relatively weak helium-like spectroscopic features measured. It is now necessary to determine the dimensionless parameters; ξ and the Mach numbers should be as large as possible and must exceed unity, whilst β and Eu need to be matched between the SNR and experiment.

As pointed out earlier, the counter-streaming experiments indicate that the ion (and electron) MFP far exceeds the experimental size (1 mm). The inferred collisionality ($\xi \sim 300$) exceeds unity. There is no evidence of electrostatic instabilities resulting in a collisionless coupling between the counter-streaming particles [16].

We discuss matching β first as this acts to localise ions and electrons on length-scales below the MFP's. If the particles are localised, we treat the plasma with an effective collisional length of order the particle Larmor radii and a fluid description of the experiment, using MHD for example, can be applied. However, in these experiments the magnetic field must penetrate fully ionised, supersonic plasma. This is an area of much uncertainty. The experimental data presented in Figs. 2c and 2d indicate that the magnetic field plays a role in the interaction of the counter-streaming plasmas, yet data presented in Fig. 2a indicates that this magnetic field does not directly affect the plasma expansion. Possible explanations are that the magnetic field is pinched between the plasmas, or that the field has penetrated the plasmas. Experiment shows that the magnetic field does not decelerate the expanding plasma. However, the modified n_e profile with steep gradients close the foil target surface and an extended low density plateau may be due to retarded bulk plasma flow occurring in the counter-streaming experiments. Cold, high charge-to-mass ratio H^+ ions pulled from the plasma by the hot and more mobile electrons stream ahead of the plasma bulk and 'push' against the inflow of the opposing plasma. This situation requires that the H^+ ions be localised, probably by the magnetic field.

A mechanism for magnetic field penetration based on ion-acoustic turbulence [21] is proposed [16]. The turbulence is induced by a skin current that tries to exclude the strong external magnetic field when the drift velocity exceeds the local sound speed. This leads to an anomalous resistivity through enhanced electron scattering, and

subsequent magnetic field penetration. Applying this model whilst accounting for the temporal development of the exploding plasma up to 500 ps, indicates that at 500 ps the magnetic field can diffuse [22] to within 300 μm of the foil target surface. The relevant plasma β is a non-standard parameter based on the plasma flow kinetic energy and not the thermal kinetic energy. The plasma β is adjusted by altering the magnetic field strength, the density, or flow speed of the plasma. Experiment tends to be constrained to the highest flow speeds and magnetic fields. A high flow speed ensures a collision-free interaction and that the experimental β remains high. At 500 ps with the largest externally applied magnetic field of 7.5 T, $\beta \sim 500$. In addition, the high magnetic field is needed to localise the counter-streaming ions and electrons such that the MHD approximation can be applied. A magnetic field of 7.5 T field induces an ion and electron effective collisionality of 10^{-1} and 10^{-3} respectively. These estimates are based on magnetic field penetration and ion and electron temperatures of 180 ± 20 eV extracted from the Doppler broadened C^{4+} transitions and Faraday cup measurements. The plasma flow speed should be included; this increases the ion Larmor radius to approximately the experiment size. In this case the ions are poorly localised.

Our experimental approach is to converge on the conditions typical of a SNR shock at 100 years after the supernova event. The emphasis is on creating a scaled snapshot and diagnosing the physical processes occurring in such plasma. This is achieved by matching the Euler number, *Eu*. This match is achieved by determining the plasma density, which is readily adjusted though a combination of laser intensity, target thickness, and target foil separation. Using the nominal experimental parameters of 100 nm thick foil targets separated by 1 mm and irradiated with a 5×10^{13} W/cm^2 in a 80 ps 1053 nm laser pulse the experiment converges to an $Eu = 21$ at 500 ps.

Finally, the supersonic flow, which is typical of these cool ablating plasmas [23], indicates that the experimental approach is a good candidate for strong shock formation. However, this relies on a strong interaction between the counter-streaming plasmas. While the ion localisation, which depends on the experiment size, the magnetic field strength and penetration, is not small enough to result in a shock, magnetic field penetration may have caused the density features presented in Fig. 2d. Unfortunately, magnetic field strength, plasma density, and size of the experiment prevent direct measurement of the penetrated field. The issue of field penetration must be addressed in future experiments.

SIMULATIONS

Hydrodynamic simulations accurately reproduce the single exploding plasma time-dependent n_e profiles. This is due to the low ion temperatures (of order 100 eV) which ensure that the exploding plasmas are collisional. It is the interaction of the two exploding plasma that is collisionless. Using hydrodynamic simulation, fitted to measurement, we are able to examine how the scaling parameters may vary with space and time. Med103, a one-dimensional laser-plasma Lagrangian, hydrodynamics model is used. The numerical simulation uses an 80 ps 5×10^{13} W/cm^2 pulse and a Thomas-Fermi equation of state with flux limited electron and ion heat transport, the flux limiter is set to 0.1. The modeling results for single foil targets, compared to selected

experimental results, are shown in Fig. 3. First, we show that the plasma flow at the experimental mid point (0.5 mm) remains strongly supersonic for at least 2 ns. This is due to the high flow speed and relatively low electron temperature (the sound speed scales as the root of the electron temperature); note that the ion temperature is

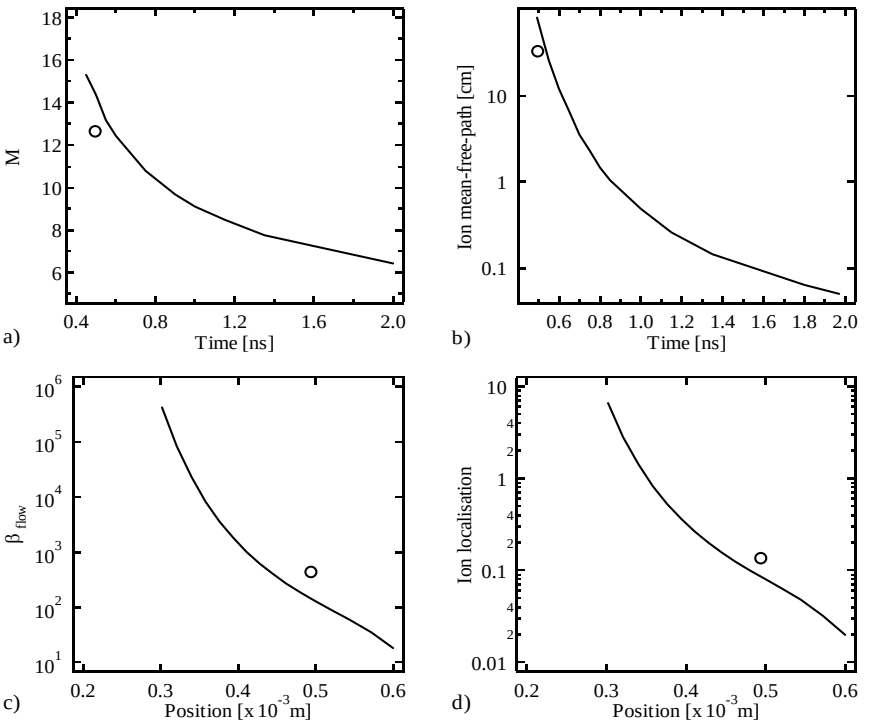

FIGURE 3. Inferred experimental measurements (open circles) at 0.5 mm and 500 ps are compared to in a) and b) the calculated time dependent Mach number (M) and the C^{6+} counter-streaming mean-free-path respectively at 0.5 mm, and in c) and d) the calculated position dependent flow plasma-β, and ion localization respectively at 500 ps.

expected to increase dramatically on shock formation [9]. As illustrated in Fig. 3b the C^{6+}, at 0.5 mm and 500 ps, the counter-streaming ion interaction is collision-free plasma. This is expected to change rapidly in time as higher density plasma with lower flow speed moves into the central region of experiment. At approximately 1.6 ns the MFP is of the order the experiment size, i.e. 1 mm. By applying the anomalous resistivity model discussed above to the numerical simulations, at say 500 ps, it is possible to examine the potential influence of the magnetic field on the plasma. The calculations shown in Figs. 3c and 3d are based the calculated time-dependent n_e profile and a fast magnetic field diffusion model [22]. It is found at 500 ps that magnetic field penetration can occur to within 0.3 mm of the foil target surface. Based on these assumptions it is found that the flow pressure exceeds the magnetic pressure (i.e. the flow plasma-$\beta > 1$) throughout the exploding plasma. The ion localization, as

discussed earlier and illustrated in Fig. 3d is more problematic. To ensure that plasma exhibits fluid-like behaviour the particle Larmor radii must be small compared to the length scales of interest, i.e. ion localization << 1. This is the case for the low mass electrons.

MAGNETIC FIELD GENERATION

Two methods can be employed to increase the ion localization. Either increase the plasma size relative to the particle Larmor radii, or decrease the Larmor radius. Plasma size is usually limited by the facilities and experimental geometry available. The approach explored here is the generation of strong magnetic fields. The Bitter magnet used in these experiments is capable of 13 T peak field, but was limited due to electrical breakdown problems to 7.5 T in the vacuum environment. Bitter magnets can produce fields exceeding 30 T; however the infrastructure required is considerable [24]. A second approach using mm-scale laser driven single turn coils [25] has been explored [16].

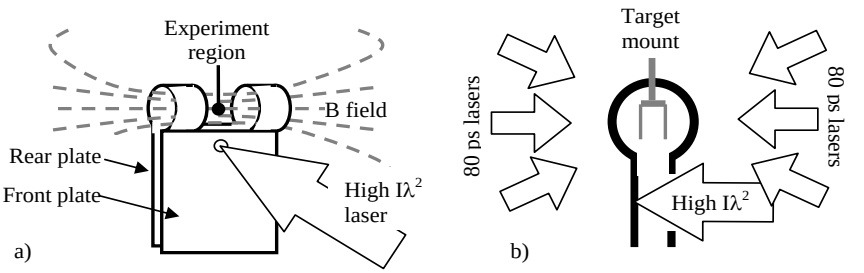

FIGURE 4. The mm-scale laser driven Helmholtz coil target. a) view of the laser entrance hole in the front and the loops, b) illustrates the multi-beam, target and diagnostic accessed required. In this view the 25 ps probe images the colliding plasmas in to the page. The loop radius is 1.25 mm, and the space between the inner edges of each loop is 2.5 mm. The foil targets are mounted across a 1.1 mm diameter hole on 2 mm wide, 10 mm long copper holders. The holders are separated by 1 mm.

The method employed is to focus a high-energy, high-intensity, I, with $I\lambda^2 \sim 10^{16}$ W/cm^2.μm^2 on to a plate and produce a hot (> 10 keV) electron source. The hot electrons induce a potential difference on a second plate placed face parallel. If the two plates are connected by a wire, a strong reverse current may pass through the wire and generate a magnetic field. Due to the need for uniform magnetic fields and access to the experiment with six laser beams, a probe beam, and target mount, a Helmholtz coil geometry is used. The Helmholtz coil target, beam, and diagnostic access are shown in Figs. 4a and 4b respectively. The foil targets are placed between the Helmholtz coil target loops.

The Helmholtz coil target is constructed in one piece from a photo-etched 50 μm thick copper sheet. Two 750 μm wide copper ribbons separated by 2.5 mm connect the two 8 × 4 mm rectangular plates. The ribbons are then bent to form two 1.25 mm radius circular loops concentric along a single axis; the plates are positioned to ensure they are face parallel and separated by 500 μm. A 1 ns duration, 300 J, 1053 nm laser pulse focused to 4 × 10^{16} W/cm^2 passes through a 500 μm diameter hole drilled into

the front plate and strikes the rear plate. Approximately 10% of the electrons in the plasma have temperatures exceeding 10 keV. These hot electrons stream down the electron density gradient ahead of the plasma plume to the front plate. A large electrical potential (~200 kV) develops between the plates, which drives a reverse current through the wire loops. This reverse current creates the magnetic field used in experiments. The magnetic field is measured with a series of calibrated single-turn 1 mm diameter screened induction coils coupled to a 4 GHz bandwidth digital oscilloscope that records the temporal variation of the signal. These induction coils are used to infer a peak magnetic field of 7 T in the central region of the Helmholtz coil target, with a field decay of 17 ns. The hot electron temperatures, inferred from the hard X-ray bremsstrahlung spectrum was ~15 keV. These results are used to develop a simple model of the Helmholtz coil target. This model suggests that designs can be optimized to produce 30 T magnetic fields with Helmholtz coil configuration, and above 100 T for single loops targets.

Colliding plasma experiments have been performed using these Helmholtz coil targets, producing data in agreement with data presented in Fig. 2. Target design is easier, and beam and diagnostic access is improved with these targets, however experimental reliability is poor. Furthermore, there is a delay of ~ 2 ns before the peak field is reached. At peak field the exploding plasmas are formed, by this time Cu plasma from the Helmholtz coil target has entered the experimental area between loops and obstructs the exploding plasma interaction.

CONCLUSION

These experiments indicate that the necessary requirements for a laboratory study of collisionless physics relevant to a young SNR can be achieved using a laser-plasma experiment. This is determined by identifying a suitable plasma model (in this case MHD) and matching a set of scaling parameters (ξ, plasma-β, Eu, M, and M_A) believed typical of the SNR in the laboratory. Despite the enormous difference in physical scales, carefully designed laboratory plasma systems can and have exploited fundamental similarities with astrophysical plasmas. We have explored the counter-streaming interaction of two supersonic highly ionised plasmas in a transverse magnetic field. A magnetic field driven interaction has been observed, although there is no evidence for a shock. Currently, the greatest limitation is the ratio of the particle (in particular the ion) Larmor radius to the size of the experiment. This ratio, the ion localisation, is somewhere between 0.1 and 1. It is believed an ion localisation of 0.01 is required. This may be achieved by working with both large magnetic fields, 30 T seem plausible, and large experimental plasmas, of the order 1 cm. This will require working with lower plasma density to ensure the collisionality parameter remains sufficiently high. These requirements are demanding yet possible with current technology.

ACKNOWLEDGMENTS

We express our thanks to the Central Laser Facility staff for supporting these experiments and in particular Martin Tolley for the careful design and production of the Helmholtz coil targets. This work is funded by the UK Engineering and Physical Sciences Research Council.

REFERENCES

* Current address: CEA Bruyeres Le Chatel, BP12, 91680 Bruyeres Le Chatel, France.
[1] J. M. Dawson, *Phys Fluids* **7**, 981 (1964).
[2] B. H. Ripin, C. K. Manka, T. A. Peyser, E. A. Mclean, J. A. Stamper, A. N. Mostovych, J. Grun, K. Kearney, J. R. Crawford and J. D. Huba, *Laser Part. Beams* **8**, 183 (1990).
[3] B. A. Remington, D. Arnett, R. P. Drake and H. Takabe *Science* **248**, 1488 (1999).
[4] H.Takabe, *Prog. Theor. Phys. Supp.* **143**, 202 (2001).
[5] J. W. Connor and J. B. Taylor, *Nucl. Fusion* **17**, 1047 (1977).
[6] D. D. Ryutov, B. A. Remington and H. F. Robey. *Phys. Plasmas* **8**, 1804 (2001).
[7] A. C. Calder, B. Fryxell, T. Plewa, R. Rosner, L. J. Dursi, V. G. Weirs, T. Dupont, H. F. Robey, J. O. Kane, B. A. Remington, R. P. Drake, G. Dimonte, M. Zingale, F. X. Timmes, K. Olson, P. Ricker, P. MacNeice and H. M. Tufo, *Astrophys. J. Suppl*. S **143**, 20 (2002).
[8] N. C. Woolsey, C. Courtois, and R. O. Dendy, *Plasma Phys. Contr. Fusion* **46,** B397 (2004).
[9] N. C. Woolsey, Y. A. Ali, R. G. Evans, R. A. D. Grundy, S. J. Pestehe, P. G. Carolan, N. J. Conway, R. O. Dendy, P. Helander, K. G. McClements, J. G. Kirk, P. A. Norreys, M. M. Notley and S. J. Rose, *Phys. Plasmas* **8**, 2439 (2001); ibid *Phys. Plasmas* **9**, 729 (2002).
[10] C. Courtois, R. A. D. Grundy, A. D. Ash, D. M. Chambers, N. C. Woolsey, R. O. Dendy, K. G. McClements, *Phys. Plasmas* **11**, 3386 (2004).
[11] Y. P. Zakharov, *IEEE T Plasma Sci* **31**, 1243 (2003).
[12] R. P. Drake, *Phys. Plasmas* **9**, 727 (2002).
[13] J. E. Borovsky, M. B. Pongratz, R. A. Rousseldupre and T. H. Tan, *Astrophys. J.* **280**, 802 (1984).
[14] R. P. Drake, *Phys. Plasmas* **7**, 4690 (2000).
[15] A. Decourchelle, D. C. Ellison, J. Ballet, *Astrophys. J.* **543,** L57 (2000).
[16] C. Courtois, A. D. Ash, D. M. Chambers, R. A. D. Grundy, N. C. Woolsey, *J. Appl. Phys.* **98**, (2005).
[17] N. J. Peacock and B. A. Norton, *Phys. Rev.* A **11,** 2142 (1970).
[18] S. N. Dixit, I. M. Thomas, B. W. Woods, A. J. Morgan, M. A. Henesian, P. J. Wegner and H. T. Powell, *Appl. Optics* **32**, 2543 (1993).
[19] N. C. Woolsey et al. to be published.
[20] C. D. Gregory, A. D. Ash, D. M. Chambers, C. Courtois, R. A. D. Grundy and N. C. Woolsey, *Astrophys. Space Sci.* **298**, 389 (2005).
[21] R. M. Kulsrud *Phys. Plasma* **5**, 1599 (1998).
[22] C. E. J. Watt, R. B. Horne and M. P. Freeman, *Geophys. Res. Lett.* **29**, 1004 (2002).
[23] J. S. Pearlman and R. L. Morse, *Phys. Rev. Lett*. **40**, 1652 (1978).
[24] F. Herlach, *Rep. Prog. Phys.* **62**, 859 (1999).
[25] H. Daido, F. Miki, K. Mima, M. Fujita, K. Sawai, H. Fujita, Y. Kitagawa, S. Nakai, and C. Yamanaka, Phys. *Rev. Lett.* **56**, 846 (1986); H. Daido, K. Mima, F. Miki, M. Fujita, Y. Kitagawa, S. Nakai, C. Yamanaka, *Jpn. J. Appl. Phys*. **26**, 1290 (1987).